Off-Bottom Suspension of Thin Sheets

Pavel Ditl and E. Bruce Nauman
Isermann Dept. of Chemical Engineering, Rensselaer Polytechnic Institute, Troy, NY 12180

Much has been written about suspension in agitated tanks; however, the results differ with respect to scale-up predictions and the the effects of particle diameter, viscosity and solid concentration. Most studies are on spherical particles or granular materials such as sand; suspension studies for nonspherical particles are very rare. Tay et al. (1984) investigated the suspension of large cylinders. Chapman et al. (1983) reported some data for small anthracite pellets and found that their suspension requires much higher impeller speeds than granular material of the same density. Mixing equipment manufacturers and users report serious problems with the suspension of thin, flat particles. Applications of dissolving or leaching such particles include the recycling of post-consumer commingled waste by selective dissolution and the recovery of materials from exposed photographic films.

The objectives of this study are to propose theoretical backgrounds for off-bottom suspension of thin, flat sheets in turbulent mixing and to test experimentally the effects of:

- Major particle dimension, d
- Particle thickness, δ
- Density difference, $\Delta\rho$
- Scale-up
- Impeller type
- Vessel geometry
- Solid concentration, c^v

This work also offers a correlation for the impeller speed required for off-bottom suspension, and recommendation for the design and scale-up of mixing equipment. The correlations for suspension of spherical particles recently published by Rieger and Ditl (1990) are based on a theoretical analysis and an extensive experimental program undertaken for 45°, pitched, six-blade turbines (H/T = 1, C/T = 1/2, c^v = 2.5 vol %, and blade width/D = 0.2) in baffled, cylindrical, flat-bottom tanks. For large particles, the Froude number is constant in good agreement with the theory proposed by Ditl and Rieger (1984). This also agrees with the experiments of Tay et al. (1984) for large cylinders. For smaller particles suspended under turbulent conditions, the Froude number depends strongly on the particle to vessel diameter ratio, d/T.

P. Ditl is presently at the Department of Chemical and Food Engineering, Czech Technical University, Technicka 4, 16607 Prague 6, Czechoslovakia.

Theoretical Approach

We adapted and perfected the theoretical approach of Rieger and Ditl (1990) proposed for spherical and granulated particles, which is based on inspection analysis of the governing equations. Focusing our attention to the most important hydrodynamic region of turbulent Reynolds number, we can describe the suspension of thin, flat particles by the following equations.

Liquid phase

At high impeller Reynolds numbers, $Re > 25{,}000$, the Navier-Stokes equation can be written in dimensionless form as:

$$\frac{D\vec{u}^*}{Dt^*} = -\nabla^* p^* \tag{1}$$

where

$$u^* = u/ND \qquad p^* = p/\rho N^2 D^2$$
$$t^* = Nt \qquad \nabla^* = D\nabla$$

The continuity equation can be written as:

$$\nabla^* \cdot \vec{u}^* = 0 \tag{2}$$

Particle

The momentum balance for a motionless, suspended particle can be written as:

$$\frac{\rho N^2 D}{\Delta\rho g} \nabla P^* = \vec{g}^* \tag{3}$$

where the modified pressure $P = p + \rho g z$ represents the pressure arising solely from fluid flow. This expression is used widely in the fluidization literature and shows an explicit dependence on the Froude number. Equations 1 and 2 introduce no dimensionless parameters directly, but a second dimensionless group is introduced through the boundary conditions. This may be seen from a force balance on a particle:

$$Vp\Delta\rho\vec{g} = -\int_{A_p} \vec{n}\, pdA_p + \int_{A_p} n \cdot \vec{\tau}\, dAp \tag{4}$$

where

$$\vec{\bar{\tau}} = \mu[\nabla \vec{u} + (\nabla \vec{u})^T]$$

is the dynamic stress tensor.

At high Reynolds numbers, the friction term can be neglected, and Eq. 4 can be rewritten in the following dimensionless form:

$$V_p^* g^* = -\frac{\rho N^2 D^2}{\Delta\rho g \delta} \int_{A_p^*} \vec{n}\, p^* dA_p^* \tag{5}$$

where

$$V_p^* = V_p/\delta d^2 \qquad A_p^* = A_p/d^2 \qquad g^* = \vec{g}/g$$

For isolated particles in geometrically similar vessels (constant T/D, C/D, H/T, baffle and vessel geometry), the following equation describing the state of particle suspension can be drawn from Eqs. 1, 2 and 5:

$$Fr = f_1(Fr_p) \tag{6}$$

where

$$Fr = \frac{\rho N^2 D}{\Delta\rho g}$$

and

$$Fr_p = \frac{\rho N^2 D^2}{\Delta\rho g \delta} = Fr \cdot \frac{D}{\delta}$$

For geometrically similar vessels, the dependence on D/δ is equivalent to a dependence on δ/T. Thus, Eq. 6 can be rewritten as:

$$Fr = f_2\left(\frac{\delta}{T}\right) \tag{7}$$

The dependence of Fr on δ/T must be determined experimentally.

The minimum impeller speed for suspension, N_s, is usually defined as the speed at which no particle remains on the vessel bottom for more than one second. It follows from Eq. 7 that N_s is not affected by the fluid viscosity or by the major particle dimension when low concentrations of thin, flat particles are suspended in a turbulently agitated tank.

Equations 1 and 5 are valid for each particle. The number of particles can be expressed as:

$$i = \frac{c^v V}{V_p} = \frac{\pi}{4} \frac{T}{\delta} \cdot \left(\frac{T}{d}\right)^2 \tag{8}$$

From Eq. 8 it follows that at higher solid concentrations, the Froude number might depend on d/T, as well as on δ/T. Our experiments did not reveal this dependence however. Equation 7 can be expressed in terms of specific power input ϵ[W/m^3]:

$$\epsilon_s \left(\frac{\rho}{D(\Delta\rho g)^3}\right)^{1/2} = f\left(\frac{\delta}{T}\right) \tag{10}$$

Specific power input ϵ can be determined from the following equation:

$$\epsilon_s = \frac{P}{V} = \frac{4 P_o \rho_{sus}}{\pi} N_s^3 D^2 \left(\frac{D}{T}\right)^3 \tag{11}$$

which was derived assuming a liquid height equal to the vessel diameter. The value of the power number, P_o, can be obtained from standard correlations of P_0 vs. Re, and ρ_{sus} is the suspension density usually calculated as the mean suspension density or more accurately, as the suspension density close to the impeller that requires the knowledge of the solid-phase distribution. The most accurate way of determining ϵ is, of course, to measure P directly. Equation 11 allows the comparison of different vessel geometries and impeller types from the viewpoint of energy consumption.

Experimental Studies

The experiments were carried out for classical mixing geometries, as shown in Figure 1. The axial flow impellers pumped downward. The blade width was 0.2 D for both the 45° pitched six-blade and flat six-blade turbines. It was slightly different from the classical geometry in that the baffles extended only to lower edge of the impeller. This arrangement has a positive effect on particle suspension and decreases the minimum impeller speed for suspension by about 10% compared to baffles that extend to the vessel bottom. Based on previous experience, the standard impeller clearance was $C/D = 2/3$ for both axial impellers and $C/D = 1/3$ for the radial impeller. The tank of diameter $T = 295$ mm was mixed using a Servodyne Mixer Controller, Model 500000-00 marketed by Cole-Parmer Instrument Co., which is equipped with a torque meter. The minimum impeller speed was defined visually as that speed where no particle remained on the vessel bottom for more than 1 second.

Results

The turbulent values of power number, P_o, for liquid mixing were evaluated from the torque measurements. Their values are listed in Table 1 for all three impellers. The value 0.45 for A310 is higher than that of 0.3 reported by the manufacture, but the others are in very good agreement with published data. The most plausible explanation of this discrepancy is a possible slight difference in standard impeller geometry, or less plausibly, the effect of baffles or impeller clearance. The values in Table 1 were used to calculate the specific power input ϵ using Eq. 11. It is fair to note that the same values of ϵ evaluated from the torque measurements are at higher solid concentrations significantly higher (up to three times) and high torque fluctuation were also observed. A similar phenomenon was reported by Novak and Rieger (1971) who found that the power

Table 1. Turbulent Values of Power Number for Liquid Mixing

Impeller Type	C/D	P_o
45° Pitched 4-Blade Turbine	2/3	1.35
Lightnin A310	2/3	0.45
Flat 6-Blade Turbine	1/3	4.8
	2/3	3.7

Mixing Equipment

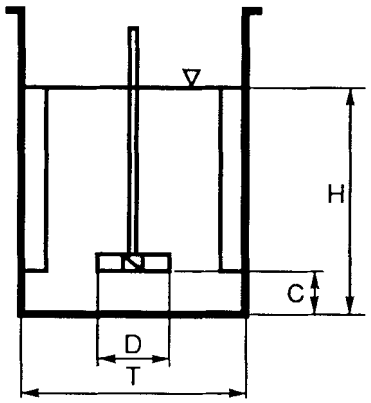

Vessel to impeller geometry: H/T = 1, T/D ≃= 3, C/T = < 1/3 - 1 >
cylindrical flat bottom vessel
T = 295, 440 mm
four baffles of width 0.1 T

Impeller Types:

45° pitched four blade turbine	D = 102, 152.4 mm
Lightnin A310	D = 96, 152.4 mm
Flat six blade turbine,	D = 97 mm

The authors are grateful to Lightnin Co. for donation of the impellers

Figure 1. Vessel and impeller geometries.

number of suspension mixing depends on the ratio of particle to tank diameter, particularly for large particles. To be consistent with their results, we can only speculate that the observed increase in power input will be much less pronounced in large tanks for which the ratio d/T falls within the applicability of Eq. 11. A deeper understanding of this phenomenon requires further study.

Thin, flat sheets

The effect of the relative major particle dimension, d/T, was tested as a next step. Experiments were carried out with PVC disks and square-shaped particles of thicknesses, $\delta = 0.5$, 0.8 and 2.5 mm at solid concentrations of ~0, 0.1 and 0.5 wt. %. The major particle dimension ranged from 4 to 13.4 mm. Measurement was carried out in the smaller vessel, $T = 295$ mm, using all three impellers, as shown in Figure 2. In agreement with Eq. 7, we found no effect of the relative major particle dimension on the minimum impeller speed for suspension, N_s, within the range of measurements and limits given by the accuracy of the visual method. We observed no significant difference in N_s for disks and squares having the same thickness. On the other hand, the effect of particle thickness was evident and therefore attention was focused on this parameter.

Figure 3 shows the dependence of N_s on the particle thickness of PVC and aluminum disks of $d = 13.5$ mm. As suggested by Eq. 7, we plotted the data obtained using particles of different materials suspended in both size vessels on one graph of Froude number vs. the relative particle thickness δ/T. Figure 3 shows the results for all three impellers using standard impeller clearances at a solids concentration of 0.1 wt. %. This graph is very similar to that in Rieger and Ditl (1990) obtained for spherical particles. Note, however, that δ/T replaces d/T. N_s increases up to a critical value, $(\delta/T)_{CR}$, and then remains constant.

The same method of data analysis was applied to higher solids concentrations with the surprising result that N_s did not appear to depend on δ/T over the entire experimental range.

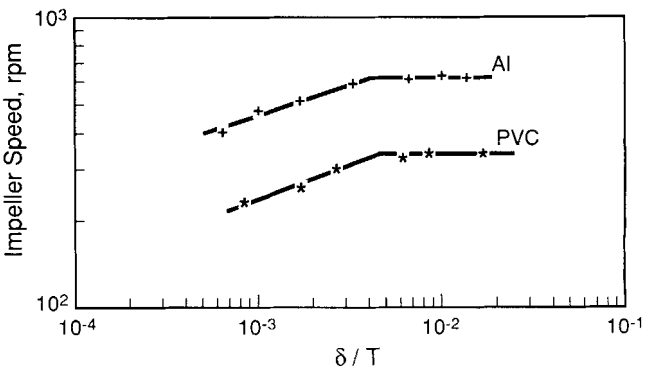

Figure 2. Minimum impeller speed for suspension vs. relative particle thickness, PVC and Al disks, $d = 13.7$ mm, Lightnin A310 impeller, $T = 295$ mm, solids concentration, 0.1 wt. %.

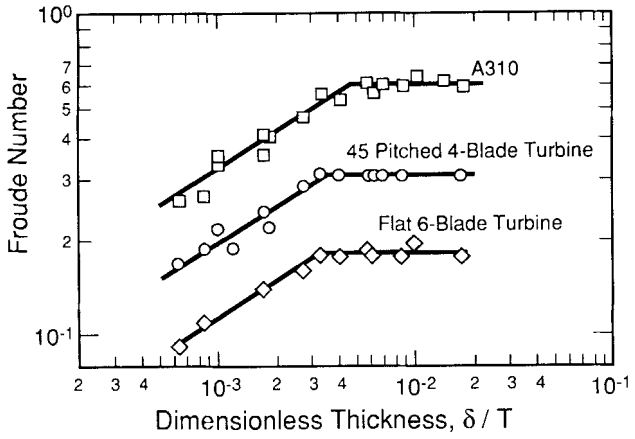

Figure 3. Suspension of flat, thin nonagglomerating particles.

Solids concentration 0.1 wt. %, solid points - $T=0.44$ m, disks $d=13.7$ mm, empty symbols-$T=0.295$ m.

The open points in Figure 4 show this behavior. Visual observation of the suspension showed that the thin, flat plastic sheets tend to agglomerate on their flat side, as shown in Figure 5. In this way, the effective thickness increases, and the condition for suspension of such particles is the same as that for single particles of thickness, which is equal to or larger than $(\delta/T)_{CR}$. The solid points in the Figure 6 show that the single-particle dependence of Fr on δ/T can be retained when agglomeration is supressed (for example, by additives or shear stress) or nonagglomerating systems (for example, particles with rough surfaces or systems with convenient electrical properties). For the data in Figure 4, agglomeration was depressed by judicious choice of materials.

Only one of parameters preventing particle agglomerization, namely shear stress at the vessel bottom, can be affected by the design of the mixing apparatus. Intensive energy dissipation at the bottom is desirable and can be increased by decreasing the impeller clearance. An increase in the tangential velocity at the bottom can also significantly improve the situation in the corner between the vessel wall and bottom. From these

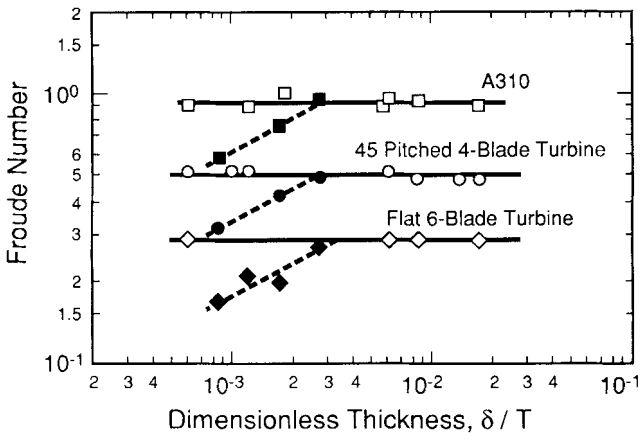

Figure 4. Suspension of flat, thin sheets creating agglomerated (empty symbols) and nonagglomerated systems (solid points).

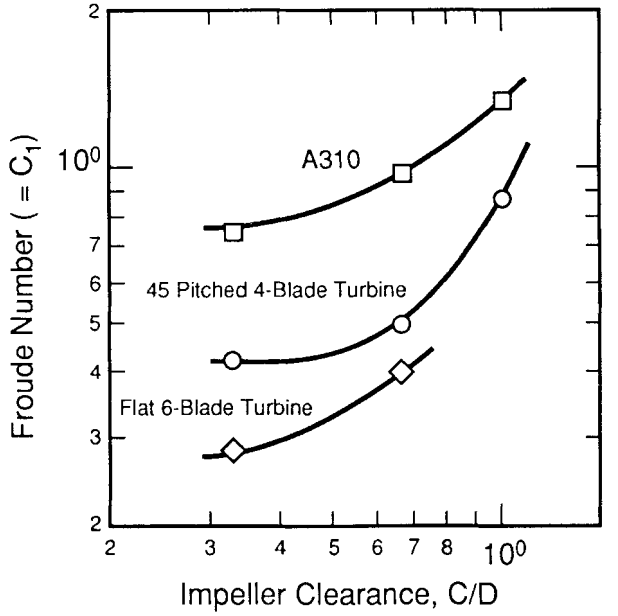

Figure 5. Effect of impeller clearance (thin, flat sheets): regime of constant *Fr*, 0.5 wt. %.

viewpoints, radial impellers should be very effective, in accordance with the practical experiences of the main manufacturers of mixing equipment. Based on the mixing hydrodynamics, we can also access the possibility of agglomeration upon scale-up. The turbulent shear stress is constant,

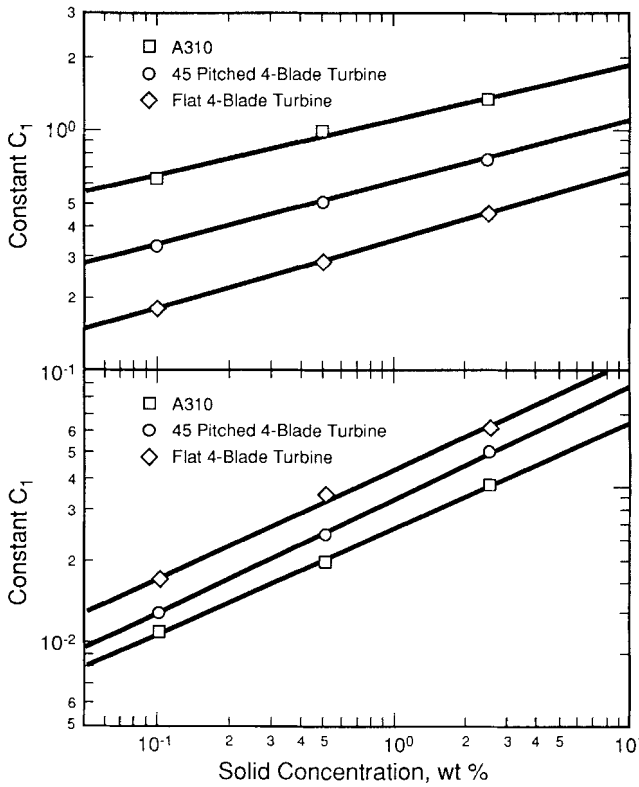

Figure 6. Effect of solids concentration on correlation constants C_1 and C_2 (thin flat sheets).

and the tangential velocity increases when scaling at constant power input per unit volume. If agglomeration is suppressed in a small vessel, it should not be a problem upon scaling. However, a complete understanding of agglomeration of large thin, flat sheets requires further study.

In accordance with Eqs. 7 and 10, our suspension of thin, flat sheets can be quantified as follows.

1. Single-particle or nonagglomerating systems:

a) Thick particles, $\delta/T > 4\times10^{-3}$

$$Fr = C_1 \tag{12a}$$

$$\epsilon\left(\frac{\rho}{\mathbf{D}(\Delta\rho g)^3}\right)1/2 = C_2 \tag{12b}$$

b) Thin particles, $\delta/T < 4\times10^{-3}$

$$Fr = C_3(\delta/T)^{0.4} \tag{13a}$$

or

$$\epsilon\left(\frac{\rho}{\mathbf{D}(\Delta\rho g)^3}\right)1/2 = C_4(\delta/T)^{0.6} \tag{13b}$$

2. Multiple-particle agglomerating systems:

which are identical with Eq. 12.

Values of the constants C_1, C_2, C_3, and C_4 are given for different impeller clearances, solid concentrations, and impeller types in Table 2. Applicability of these constants was proved for the range specified by the following characteristic parameters: $0.007 < \delta/d < 0.2$; $0.001 < \delta/T < 0.02$; $Re > 25{,}000$; $0.4 < \Delta\rho/\rho < 1.7$, $3\times10^5 < Ar < 10^7$.

To show the effects of the individual parameters on the minimum impeller speed required for particle suspension, it is useful to rewrite Eqs. (12a) and (13a) in their dimensional forms.

1. Single-particle or nonagglomerating systems:

a) Thick particles

$$N_s = C_1\delta^0 T^{-0.5}\Delta\rho^{0.5} \tag{14}$$

b) Thin particles

$$N_s = C_3\delta^{0.2}T^{-0.7}\Delta\rho^{0.5} \tag{15}$$

2. Multiple-particle agglomerating systems:

which are identical to Eq. 12.

The cases scale differently. For thicker agglomerating particles, the scale-up rule is $N_sT^{0.5}$ = constant, and the specific power input increases with increasing vessel volume ($\epsilon_s \sim T^{0.5} \sim V^{1/6}$). For nonagglomerating, thin particles ($\delta/T < 4.10^{-3}$) the scale-up rule $N_sT^{0.7}$ = constant can be recommended, which is very close to scale-up at a constant specific power input ($\epsilon_s \sim T^{-0.1}$). The exponents (N_sT^{α} = const) obtained from our scale-up experiments made with vessels of diameters $T = 0.295$ and 0.44 m had the ranges: $0.52 < \alpha < 0.55$ for the cases 1a and 2 and $0.62 < \alpha < 0.72>$ for case 1b.

The effects of impeller clearance and solids concentration on N_s can be estimated from the constants in Table 2 assuming that $N_s \sim \sqrt{C_1} \sim \sqrt{C_3}$ or $\epsilon_s \sim C_2 \sim C_4$. Figure 5 shows the effect of impeller clearance for the three impellers with 0.5 wt. % suspensions. It is seen that both axial impeller types should be operated at $1/3 < C/D < 2/3$ where the plot of Fr vs. C/T is rather flat. The plot for the radial impeller is steeper, supporting our choice of the standard clearance $C/D = 1/3$. Figure 6 shows the effects of solids concentration on the constants C_1 and C_2. At the lower concentrations, the logarithmic plots are the straight lines from which we conclude that $N_s \sim X^{0.15}$, in good agreement with most other authors. The plot for C_2 allows the efficiency of the impellers to be compared since, as indicated above, $C_2 \sim \epsilon$. The most efficient impeller is A310 followed by the 45° pitched blade turbine and then the flat six-blade turbine.

The experimental data of Tay et al. (1984) for suspension of aluminum and large steel cylinders using a 45° pitched four-blade impeller can be evaluated using the concepts described in this work. For $X = 0.012$ wt. %, we find $C_1 = 0.15$ compared to $C_1 = 0.31$ as listed in Table 2 for the same impeller, $C/D = 2/3$ and $X = 0.01$ wt. %. The 100% difference in Froude number reflects a 40% difference in the impeller speed required for suspension. Five percent of this difference is due to a difference in T/D ratio (2.9 and 2.95), the rest is presumably due to different bottom configurations. Tay et al. used a dished

Table 2. Values of Constants in Eqs. 12a, 12b, 13a and 13b for Thin, Flat Sheets

Impeller Type	C/D	wt. %	C_1	C_2	C_3	C_4
45-Pitched 4-Blade	1/3	0.1	0.25	0.009		
Turbine		0.5	0.42	0.020		
		0.1	0.31	0.013	3.0	0.38
	2/3	0.5	0.50	0.026	5.0	0.81
		2.5	0.75	0.047		
$T/D = 2.9$		0.1	0.54	0.029		
	1	0.5	0.94	0.066		
Lightnin A310	1/3	0.1	0.52	0.0076		
		0.5	0.74	0.013		
$T/D = 3.07$		0.1	0.61	0.0098	5.3	0.25
	2/3	0.5	0.95	0.019	9.6	0.61
		2.5	1.23	0.028		
		0.1	0.74	0.013		
	1	0.5	1.3	0.030		
Flat 6-Blade Turbine		0.1	0.18	0.017	1.8	0.53
	1/3	0.5	0.29	0.035	2.9	1.09
		2.5	0.43	0.062		
$T/D = 3.04$		0.1	0.30	0.028		
	2/3	0.5	0.40	0.043		

bottom tank with an inverted cone below the impeller to improve the flow pattern. We used a standard flat bottom vessel, which is not so ideal for suspension. Accuracy limits of 10% are due to the subjectivity of visual observation.

Thin, Curved Sheets

One application of a suspension of thin sheets is to recycle post-consumer commingled plastic waste by selective dissolution (Lynch and Nauman, (1989). In this technology, the concentration of shredded plastic materials should be as high as possible. To extend our results to this application, a set of suspension experiments with shredded PET was carried out in both vessel sizes with up to 15 wt. % of thin, curved particles. The particles were formed by shredding PET bottles. The polydisperse mixture consisted of particles having thickness $\delta = 0.8$ mm and with a curved major dimension ranging from 4 to 20 mm. Based on visual observations, the curved, irregular particle shape eliminated agglomeration. The calculated values of Froude number for the lower particle concentrations of 0.1 and 0.5 wt. % agreed surprisingly well with the results obtained for nonagglomerating thin, flat particles. Therefore, we decided to intercept the results obtained with curve-shaped particles the same way as for thin, flat, nonagglomerated particles, in term of Eqs. 13a and 13b. The constants C_3 and C_4 are plotted in Figure 7. The results obtained with both vessel sizes fall reasonably well on one plot, supporting our method of analysis. There exist definitely limits of the applicability of this approach with respect to particle shape and solid concentration, which must be verified experimentally. It should be also reminded that $N_s \sim C_3^{0.5}$ and $\epsilon_s \sim C_4$. From Figure 7 it follows that suspension of curve-shaped particles is less concentration-dependent at lower concentrations $N_s \sim X^{0.09}$; however, a drastic increase of N_s with an increase of solid concentration above 5 wt. % is evident. Figure 7 also allows a comparison of the impeller types from the viewpoint of energy consumption ($\epsilon_s \sim C_4$). The difference between the impellers is more pronounced at lower solid concentrations, whereas at higher concentrations the difference is much smaller and even an inversion in efficiency of the axial impellers was found.

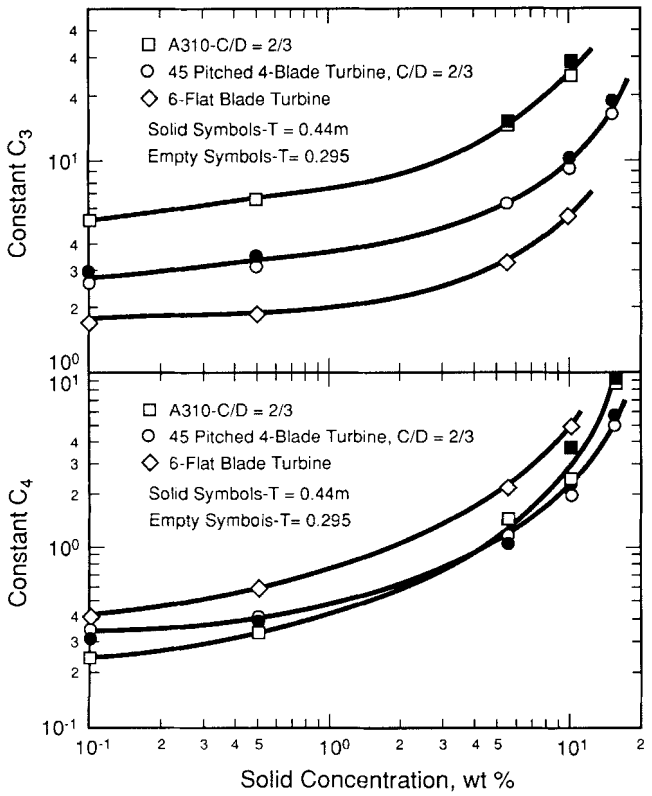

Figure 7. Effect of solids concentration on correlation constants C_3 and C_4 (thin curved sheets.)

Notation

A_p = particle surface, m^2
Ar = Archimedes number = $d^3\rho(\Delta\rho g)/\mu^2$
B = width of the baffles, m
C = impeller clearance, m
C_1, C_2, C_3, C_4 = constants in Eqs. 12a, 12b, 13a and 13b
C^v = volumetric particle concentration, dimensionless, vol. %
d = major particle dimension, sphere diameter, m
D = impeller diameter, m
Fr = Froude number = $N^2D\rho/\Delta\rho g$, dimensionless
Fr_p = particle Froude number = $\rho N^2D^2/\Delta\rho g\delta$, dimensionless
g = acceleration due to gravity, m/s^2
H = liquid high, m
i = number of particles, dimensionless
$\vec{n}$ = unit normal vector
N = impeller speed, rps, rpm
N_s = impeller speed required for particle suspension, rps, rpm
p = pressure, Pa
P = power input, W
p_m = modified pressure defined as $p+\rho gz$, N/m^2
P_o = power number, dimensionless
Re = impeller Reynolds number = $ND^2\rho/\mu$, dimensionless
t = time, s
T = tank diameter, m
u = liquid velocity, m/s
V = suspension volume, m^3
V_p = volume of one particle, m^3
X = weight concentration, dimensionless, wt. %

Greek letters

α = exponent
ϵ = specific power input, W/m^3
ϵ_s = specific power input for suspension, W/m^3
δ = particle thickness, m
μ = viscosity, Pa•s
ρ = liquid density, kg/m^3
ρ_s = particle density, kg/m^3
ρ_{sus} = suspension density, kg/m^3
$\Delta\rho$ = density difference = $\rho_s - \rho$, kg/m^3
$\bar{\bar{\tau}}$ = tensor of dynamic stress

Superscripts

* = dimensionless parameter
T = fluctuating turbulent velocity compound

Literature Cited

Chapman, C. M., A. W. Nienow, M. Cook, and J. C. Middleton, "Particle-Gas-Liquid Mixing in Stirred Vessels: I. Particle-Liquid Mixing," *Chem. Eng. Res. Des.*, **61**, 71 (1983).

Ditl, P., and P. Rieger, "Suspension in Agitated Suspensions," Paper V3.61, Congress CHISA, Prague (1984).

Lynch, J. C., and E. B. Nauman, "Recycling of Commingled by Selective Dissolution," *Proc. Int. Coextrusion Conf.*, p. 99 (1989).

Novak, V., and F. Rieger, "Power Input for Mixing of Grain Suspensions," *Proc. Int. Coextrusion Conf.*, in Czech, Marianske, Lazne (1976).

Rieger, F., and P. Ditl, "Suspension of Solid Particles," paper J3.3, Prague (Aug. 26–31, 1990).

Tay, M, B. Deutchlander, and G. Tatterson, "Suspension Characteristics of Large Cylinders in Agitated Tanks," *Chem. Eng. Commun.*, **29** (1984).

Manuscript received Aug. 19, 1991, and revision received Mar. 6, 1992.